Article

Climate Change Impacts on the Hydrological Processes of a Small Agricultural Watershed

Sushant Mehan [1], Narayanan Kannan [2], Ram P. Neupane [3], Rachel McDaniel [4] and Sandeep Kumar [3,*]

[1] Department of Agricultural and Biological Engineering, Purdue University, West Lafayette, IN 47906, USA; sushantmehan@gmail.com

[2] Texas Institute for Applied Environmental Research (TIAER), Tarleton State University, Stephenville, TX 76402, USA; kannan@tiaer.tarleton.edu

[3] Department of Plant Science, South Dakota State University, Brookings, SD 57007, USA; Ram.neupane@sdstate.edu

[4] Department of Agricultural and Biosystems Engineering, South Dakota State University, Brookings, SD 57007, USA; rachel.Mcdaniel@sdstate.edu

* Correspondence: Sandeep.Kumar@sdstate.edu

Abstract: Weather extremes and climate variability directly impact the hydrological cycle influencing agricultural productivity. The issues related to climate change are of prime concern for every nation as its implications are posing negative impacts on society. In this study, we used three climate change scenarios to simulate the impact on local hydrology of a small agricultural watershed. The three emission scenarios from the Special Report on Emission Scenarios, of the Intergovernmental Panel on Climate Change (IPCC) 2007 analyzed in this study were A2 (high emission), A1B (medium emission), and B1 (low emission). A process based hydrologic model SWAT (Soil and Water Assessment Tool) was calibrated and validated for the Skunk Creek Watershed located in eastern South Dakota. The model performance coefficients revealed a strong correlation between simulated and observed stream flow at both monthly and daily time step. The Nash Sutcliffe Efficiency for monthly model performace was 0.87 for the calibration period and 0.76 for validation period. The future climate scenarios were built for the mid-21st century time period ranging from 2046 to 2065. The future climate data analysis showed an increase in temperatures between 2.2 °C to 3.3 °C and a decrease in precipitation from 1.8% to 4.5% expected under three different climate change scenarios. A sharp decline in stream flow (95.92%–96.32%), run-off (83.46%–87.00%), total water yield (90.67%–91.60%), soil water storage (89.99%–92.47%), and seasonal snow melt (37.64%–43.06%) are predicted to occur by the mid-21st century. In addition, an increase in evapotranspirative losses (2%–3%) is expected to occur within the watershed when compared with the baseline period. Overall, these results indicate that the watershed is highly susceptible to hydrological and agricultural drought due to limited water availability. These results are limited to the available climate projections, and future refinement in projected climatic change data, at a finer regional scale would provide greater clarity. Nevertheless, models like SWAT are excellent means to test best management practices to mitigate the projected dry conditions in small agricultural waterhseds.

Keywords: climate change; SWAT; SRES scenarios; dry conditions; mitigation

1. Introduction

It is now beyond doubt that anthropogenic activities, including burning of fossil fuels, deforestation, and urbanization, have triggered climate change. Climate change has direct impact on

hydrological cycle which in turn starts a chain reaction impacting agriculture, energy and ecology, to name a few. The first step before planning mitigation operations is to assess the impact of climate change on water resources at both local and regional scales. Narsimlu et al. [1] carried out an assessment of climate change on Upper Sind River Basin and recorded that average streamflow could increase by 93.5% by the end of 21st century during monsoons. Similarly, Vaghefi et al. [2] concluded from their research that climate change can cause both positive and negative impact in the Karkheh River Basin in the semi-arid region of Iran. All these assessments are essential and help decision makers to take corrective decisions and formulate policies to mitigate the impact of climate change before the adversity prevails.

The issue of climate change has been studied for many large sized watersheds across the globe so far and more attention is required to assess the impact of climate change on small sized watersheds. It will then help to frame better water management startegies. It is so because the variations brought about by climate change in the local and regional hydrological regime will adversely affect the economic, social, and ecological system of the region [3]. Moreover, small agricultural watersheds, especially ones where snowmelt is an important hydrological variable, are vulnerable to variability in climate change. Previous research has shown that watersheds with more rainfall are expected to have an increase in overall flood magnitude and frequency [4,5]. However, water sources will be scarce in comparison to the present for many snowfall-dominated watersheds [6]. Such situations will lead to an era with reduced agricultural productivity, production instability, and high levels of food insecurity.

To understand the implications of climate change on the water budget, hydrologic models are gaining widespread attention. Process based models like the Soil and Water Assessment Tool (SWAT) have been used by many researchers to assess climate change impacts (e.g., [7,8] in the US, [9] in India, [10] in Kenya, and [11] in Ethopia, etc.). Gosain [12] simulated the impacts of climate change scenarios on stream flow from 2041 to 2060 for 12 major rivers basins in India using SWAT, and found that the severity of both the floods and droughts were expected to increase. It has been proved through numerous studies that SWAT is a reliable tool to assess the impact of climate change within watersheds under different climate change scenarios. Thomson [13] used SWAT to assess climate change and concluded that water yield (WYLD) changed anywhere from −210% to 77% relative to baseline levels within the entire United States.

Hydrologic models require a set of basic input, like climate data, soil data and land use data. Climate data plays an important role in deciding the simulation produced by any computer model. Future climate scenarios required for climate study are available at coarser resolution from various Global Circulation Models (GCMs), but the data needs to be finely resoluted to Regional Climate Model (RCM) scale to use them in hydrologic simulations. There is need for bias correction and downscaling while converting data from GCMs to RCMs. The overall success of the assessment of climate change studies depends on the accuracy with which the future climate data are resoluted and simulated.

This study examines the impact of climate change on the Skunk Creek, which is a small watershed located in the eastern part of South Dakota (SD), where it is being hypothesized that the climate change may cause drier conditions in the mid-21st century. To accomplish this, three different climate change scenarios were selected, representing low, moderate, and high emission scenarios, and modeled within SWAT to project the future hydrologic conditions. It is expected that changes in atmospheric circulation may contribute to changes in moisture and energy fluxes at the land surface [14]. As a result, a situation of flooding with high intensity short duration storms and a situation of droughts in absence of adequate rainfall for longer period will prevail [15]. Overall, a host of economic (losses from poor or low agricultural productivity) and social activities (shifting land use) will be disrupted if such a situation prevails in the future. Since climate change will likely persist, a better understanding of it's implications on future water budget, is a necessity [16].

2. Material and Methods

2.1. Study Site

The Skunk Creek watershed (SKW, Figure 1) located in the eastern part of South Dakota (SD), USA covers an area of 1606 km^2 and is located within 96.74° and 97.35° West and 43.45° and 44.13° North. Skunk Creek, a tributary of the Big Sioux River is a 118 km permanent natural creek that serves as an important fishing site in state and is used for many other recreational activities by local residents. It also supports agricultural activity in surrounding areas as a source of irrigation water. The land use of the study area is dominated by crop land, primarily corn (38%), soybeans (26%) and miscellaneous row crops. The soil texture is dominated by silt clay loam with a few gravelly loams; bears silt loam, loamy sand, and silt clay. The average annual rainfall is about 667.6 mm with the majority falling in the months from April to September. The average annual water yield is about 73 mm. The average daily maximum and minimum temperature values as observed after analyzing the weather data from 1980 to 2010 from Daily Surface Weather and Climatological Summaries (DAYMET) are 15.5 °C and 2.8 °C.

2.2. SWAT (Soil Water Assessment Tool) Model

SWAT model (a semi distributed hydrological model [17]) version Rev. 627 with an Arc-GIS interface was used for this study. SWAT is a versatile model that can be used to integrate multiple environmental processes, which support more effective watershed management and the development of better informed policy decisions [18]. The model has also been included in the collaborative software development laboratory that facilitates development by multiple scientists [19]. SWAT can simulate climate change impacts on plant growth, stream flow and other responses by taking into account the effect of atmospheric CO_2 concentration on plant development and transpiration [20,21]. In addition, various researchers have worked on SWAT to simulate various processes like erosion [22], sediment transport [23], and land use change [24]. In SWAT, the entire watershed is sub divided into sub basins and further into smaller units known as Hydrological Response Units (HRUs) which are based on a unique combination of soil, slope, and land use properties.

Two major phases of watershed hydrology, referred to as land phase and routing phase, are simulated in SWAT. The amount of water, sediment, nutrient, and pesticide loading to the main channel in each sub-basin is controlled under the land phase. On the other hand, movement of these materials through the channel network to the outlet is regulated by the routing phase. The land phase of the hydrologic cycle within SWAT uses the following water balance (Equation (1)) in the soil profile.

$$SW_t = SW_0 + \sum_{i=1}^{t}(R_{day} - Q_{surf} - E_a - W_{seep} - Q_{gw}) \tag{1}$$

where SW_t is the final soil water content (mm H$_2$O), SW_o is the initial soil water content (mm H$_2$O), t is time (days), R_{day} is the amount of precipitation on day$_i$ (mm H$_2$O), Q_{surf} is the amount of surface run-off (mm H$_2$O), E_a is the amount of evapotranspiration (mm H$_2$O), W_{seep} is the amount of water entering the vadose zone from the soil profile (mm H$_2$O), and Q_{gw} is the amount of return flow (mm H$_2$O) [25]. The Soil Conservation Service (SCS) curve number procedure [26] was used to calculate surface run-off which uses local land use, soil type, and antecedent moisture (Equation (2)).

$$Q_{surf} = \frac{\left(R_{day} - I_a\right)^2}{\left(R_{day} - I_a + S\right)} \tag{2}$$

where Q_{surf} is the accumulated run-off or rainfall excess (mm H$_2$O), R_{day} is the rainfall depth for the day (mm H$_2$O), I_a is the initial abstraction which includes surface storage, interception and infiltration prior to run-off (mm H$_2$O), and S is the retention parameter (mm H$_2$O). I_a is commonly approximated

as $0.2S$ [26], the surface run-off will occur when $R_{day} > I_a$. The retention parameter S was computed as presented in the Equation (3)

$$S = 25.4(\frac{1000}{CN} - 10) \tag{3}$$

where CN is the daily curve number for the day. The retention parameter which governs this value is spatially variable as it is primarily based on local land use type and soil water content [25].

For the ET computation, Hargreaves method [27] was selected, (Equation (4)).

$$\lambda E_0 = 0.0023 H_0 \times (T_{mx} - T_{mn})^{0.5} \times (T_{av} + 17.8) \tag{4}$$

where λ is the latent heat of vaporization (MJ·kg^{-1}), E_0 is the potential evapotranspiration (mm·day^{-1}), H_0 is extraterrestrial radiation (MJ·m^{-2}·day^{-1}), T_{mx} is maximum air temperature for a given day (°C), and T_{mn} is minimum air temperature for a given day (°C). This method is temperature based, but it also effectively incorporates radiation [27]. It is also expected that Hargreaves method will produce good results, because 80% of ET$_0$ can be explained by temperature and solar radiation [28]. Wang [29], during their study on hydrologic simulation on a Northwestern Minnesota watershed using different ET computation methods, reported that using the Hargreaves in SWAT was found to be slightly superior to the other two SWAT methods when computing ET.

2.3. Input Data and Model Set Up

2.3.1. Topography, Soil, and Land Use Data

The 10 m resolution digital elevation model (DEM) was obtained from National Elevation Dataset (NED) and downloaded from the geospatial data gateway. NED is a seamless raster product produced by USGS (United States Geological Survey). The land use map used in this study was of the Cropland Data Layer (CDL), produced by USDA National Agricultural Statistics Service (NASS) [30]. The CDL is a geo-referenced, crop-specific raster layer for land cover. It is created annually for continental US using moderate resolution 30 m satellite imagery and extensive ground truthing. Soil Survey Geographic Data (SSURGO) were used as the soil feature layer and was compiled by the National Cooperative Soil Survey (NCSS), USDA, and the National Resources Conservation Service (NRCS). Scales for SSURGO data range from 1:12000 to 1:63,360 [31] All the spatial datasets were set to the projections of WGS 1984 (World Geodetic System 84) UTM Zone 14 (Universal Transverse Mercator Zone 14) using ArcGIS (version 10.0) for further simulation.

2.3.2. Weather Data

Various meteorological inputs are required by SWAT, including precipitation, maximum/minimum air temperature, solar radiation, wind speed, and relative humidity. The daily observed precipitation and maximum/minimum air temperature were taken for the period from 1980 to 2000 from Daily Surface Weather and Climatological Summaries (DAYMET) Single Point Data Extraction (SPDE, http://daymet.ornl.gov/dataaccess) [32,33]. Data for five locations within the watershed (Figure 1) were used as model inputs. The dataset were available on daily time scale with the resolution of 1 km by 1 km from 1980 until the present. The source has been used by many researchers for their studies [34–36]. The remaining meteorological inputs like solar radiations, wind speed and relative humidity were automatically generated within the SWAT using weather generator input file.

2.3.3. Observed Stream Flow

The daily observed discharge data at the USGS monitoring site 06481500 (http://waterdata.usgs.gov/nwis/) located at Sioux Falls, SD for the period from 1987 to 2000 was used to calibrate the model. Calibration was carried using Sequential Uncertainty Fitting 2 (SUFI 2) algorithm within Soil

and Water Assessment Tool Calibration Uncertainty Program (SWAT CUP). Twenty-four different parameters sensitive to influence of the stream discharge with their lower and upper bound were used for calibration (Table 1).
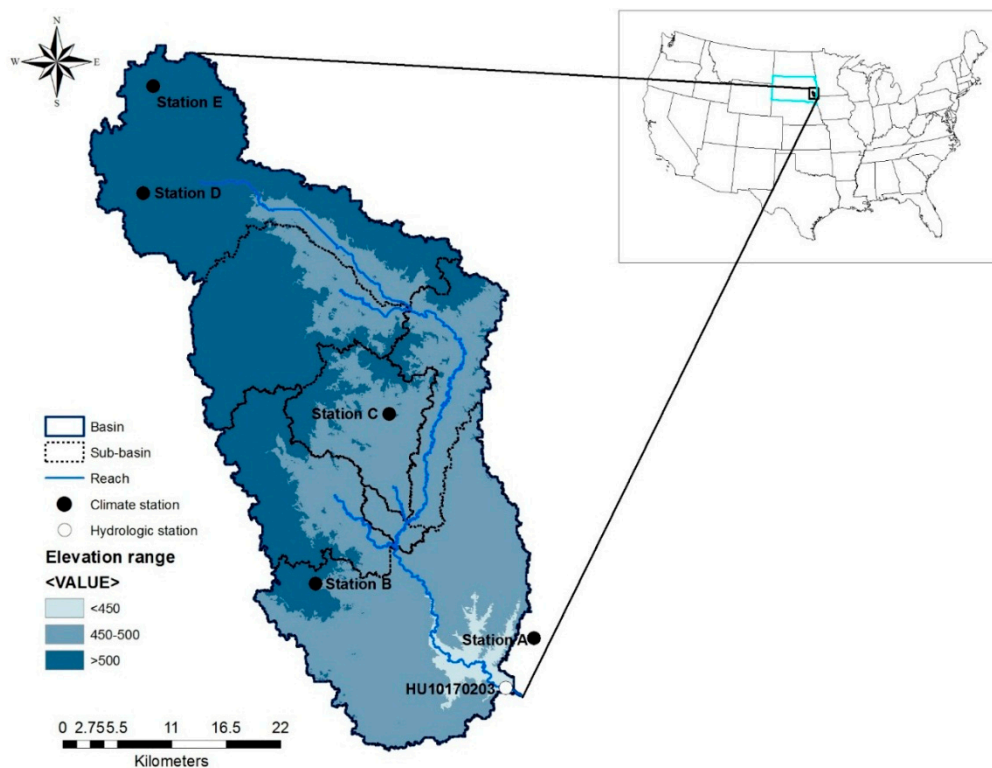

Figure 1. Delineated Skunk Creek basin using digital elevation model within soil and water assessment tool into seven sub basins with locations of climate stations (A–E) and hydrologic stations (HUC1017023).

2.4. Model Set up for Calibration and Validation

The ArcGIS interface of SWAT, Arc-SWAT was used to simulate the stream discharge for SKW. The watershed was delineated into 7 sub-basins and 364 HRUs. Simulations were run from 1980 to 2000 with a seven-year warm up period (1980–1986) that allowed the model to stabilize prior to simulation. The period from 1987 to 1994 was set as the calibration period and 1995–2000 was the validation period. Using these time periods ensured the equal distribution of high flows and low flows within calibration and validation period. Calibration was performed using SUFI 2 where Maximizing NSE (Nash Sutcliffe Efficiency) was used as the objective function. The SUFI 2 algorithm is designed so no automated optimization routine can replace the insight from physical understanding and knowledge of effects of parameters on system response [18]. Before running calibration, we analyzed the sensitivity of several parameters using a Global Sensitivity analysis (GSA). GSA involves multiple regression system, Latin Hypercube, that regresses generated parameters against objective function The algorithm was set to reduce any uncertainty and to achieve desired values of goodness of calibration (*p*-factor should be close to 1 and *r*-factor closer to zero) The values with the best fit as determined by SWAT CUP were taken and incorporated back into SWAT interface. Performance of the model was determined by the terms of coefficient of determination: R^2 (Equation (5)), Nash Sutcliffe (NSE, Equation (6)), Percent Bias (PBIAS, Equation (7)), and Root Mean Square Error (RMSE, Equation (8)).

$$R^2 = \frac{\sum_i \left[\left(Y^{obs} - Y_o^{mean} \right) \left(Y^{sim} - Y_s^{mean} \right) \right]^2}{\sum_i \left(Y^{obs} - Y_o^{mean} \right)^2 \sum_i \left(Y^{sim} - Y_s^{mean} \right)^2} \tag{5}$$

$$NSE = 1 - \frac{\sum \left(Y^{obs} - Y^{sim}\right)^2}{\sum \left(Y^{obs} - Y_o^{mean}\right)^2} \tag{6}$$

$$PBIAS = \frac{\sum \left(Y^{obs} - Y^{sim}\right)}{\sum Y^{obs}} \times 100 \tag{7}$$

$$RMSE = SQRT \left[\frac{1}{N} \sum_{i=1}^{N} \left(Y^{sim} - Y^{obs}\right)^2\right] \tag{8}$$

where, Y^{obs} and Y^{sim} are observed and simulated values of streamflow data. The optimal values recommended for the various performance statistics are, R^2 close to 1, NSE $\geq$ 0.50 and PBIAS $\leq$ 25%, and RMSE close to zero.

Table 1. Parameters and their range selected to calibrate the model using Sequential Uncertainty Fitting 2 (SUFI 2) within Soil and Water Assessment Tool Calibration Uncertainty Program (SWAT CUP), their sensitivity (*t*-stat and *p*-value determine the rank for each parameter) and best fitted value used to calibrate and validate the SWAT model.

Rank	Parameter †	*t*-Stat	*p*-Value	Best Fitted Value	Minimum Value	Maximum Value
1	R_SOL_AWC.sol	9.95	0.00	−0.05	−1.00	1.00
2	V_SMTMP.bsn	3.06	0.00	3.77	−5.00	5.00
3	R_CN2.mgt	2.34	0.01	−0.05	−0.20	0.20
4	V_EPCO.bsn	2.10	0.04	0.40	0.01	1.00
5	R_SOL_BD.sol	1.87	0.06	0.86	−1.00	1.00
6	V_SURLAG.bsn	1.85	0.07	11.66	0.00	20.00
7	V_SMFMX.bsn	1.65	0.10	6.85	1.40	7.50
8	V_SHALLST.gw	1.43	0.15	4.26	0.00	5.00
9	V_CH_N2.rte	1.26	0.21	0.15	0.01	0.15
10	R_SOL_K.sol	1.20	0.23	−0.12	−1.00	1.00
11	V_REVAPMN.gw	1.05	0.29	29.90	0.00	100.00
12	V_SMFMN.bsn	0.98	0.33	2.11	1.40	7.50
13	V_SFTMP.bsn	0.97	0.33	3.11	−5.00	5.00
14	R_OV_N.hru	0.85	0.40	0.83	−1.00	1.00
15	V_GW_DELAY.gw	0.82	0.41	449.58	30.00	450.00
16	V_CH_K2.rte	0.80	0.42	80.55	0.00	150.00
17	V_GW_REVAP.gw	0.47	0.64	0.18	0.02	0.20
18	V_GWQMN.gw	0.45	0.65	1.04	0.00	2.00
19	V_RCHRG_DP.gw	0.38	0.70	0.33	0.00	1.00
20	R_HEAT_UNITS.mgt	0.28	0.78	−0.75	−1.00	1.00
21	V_ALPHA_BF.gw	0.18	0.86	0.16	0.00	1.00
22	V_ESCO.bsn	0.12	0.90	0.95	0.00	1.00
23	V_FFCB.bsn	0.10	0.92	0.89	0.00	1.00
24	R_SLSUBBSN.hru	0.00	0.99	−0.63	−1.00	1.00

† **PARAMETRS: SOL_AWC**-Available water capacity of soil layer (mm H_2O/mm soil); **SMTMP**- Snow melt base temperature (°C); **CN2**: Initial SCS runoff curve number for moisture condition II; **EPCO**: Plant uptake compensation factor; **SOL_BD**: Moist bulk density (g/cm³); **SURLAG**: Surface runoff lag coefficient; **SMFMX:** Melt factor snow on June 21 (mm H_2O/°C-day); **SHALLST**: Initial depth of water in shallow aquifer (mm H_2O); **CH_N2**: Manning's "n" value for the main channel; **SOL_K**: Saturated hydraulic conductivity (mm/h); **REVAPMN**: Threshold depth of water in the shallow aquifer for "revap" or percolation to the deep aquifer to occur (mm H_2O); **SMFMN**: Melt factor for snow on 21 December (mm H_2O/°C-day); **SFTMP**: Snowfall temperature (°C); **OV_N**: Manning's "n" value for overland flow; **GW_DELAY**: Groundwater delay time (days); **CH_K2**- Effective hydraulic conductivity in main channel alluvium (mm/hr); **GE_REVAP**: Groundwater "revap"coefficient; **GWQMN**: Threshold depth of water in the shallow aquifer required for return flow to occur (mm H_2O); **RCHRG_DP**: Deep aquifer percolation fraction; **HEAT_UNITS**: Total heat units for cover/plant to reach maturity; **ALPHA_BF**: Base flow alpha factor (1/days); **ESCO**: Soil evaporation compensation factor; **FFCB**: Initial soil water storage expressed as a fraction of field capacity water content; **SLSUBBSN**: Average slope length (m). The extension (.hru, .bsn, .gw, etc.) refers to SWAT file type where the parameter occurs. The qualifier (V_) refers to the substitution of a parameter by a value from the given range, while (R_) refers to a relative change in the parameter were the current values is multiplied by 1 plus a factor in the given range.

2.5. Projected Climate Change Scenarios

In 1996, the Intergovernmental Panel on Climate Change(IPCC) integrated the carbon intensity of energy supply, the income gap between developed and developing country and sulfur emissions

to present a new set of scenarios in a report known as the Special Report on Emission Scenarios (SRES) [37]. Among all the SRES scenarios, four marker scenarios (A1, A2, B1 and B2) have been used most often to study the impact of climate change [38]. These scenarios include both natural and anthropogenic drivers of climate change. Out of all the emission scenarios presented in the SRES, A2, A1B, and B1 were chosen for this study. The purpose of choosing three different scenarios is that these are representative of all three extreme conditions expected in mid-21st century (High, Medium, and Low). This will help to simulate the range of possible hydrologic conditions, providing insight into the impact of climate change during the mid-21st century.

We used daily Bias-corrected Construction Analog (BCCA 3v2) average temperature and precipitation data estimated from the SRES. The data were derived for period from 2046 to 2065 with a spatial resolution of 1/8 degrees from eight different sub climatic models to maintain the consistency of the data for all the three climate change scenarios [39,40]. The bias correction followed a basic approach of smoothening monthly means (three-month running means) and based the adjustments accordingly in order to avoid abrupt discontinuity between months (i.e., to compensate for dry periods). This helped to narrow the differences and help in constructing the best fit model. Monthly "correction" ratios were derived by dividing the mean monthly observed values by the mean monthly historical BCCA projection values. These values were then applied to the BCCA projections for historical and future periods to produce corrected values. The period from 1961 to 1999 was used to develop the correction ratios for CMIP 3 (Coupled Model Projection Phase 3).

3. Results

3.1. SWAT Model Calibration and Validation

Results from the global sensitivity analysis within SUFI2 revealed that out of the 24 parameters selected for calibration, the soil available water content (SOL_AWC) (t-stat = 9.95, p-value = 0.00), snow melt base temperature (SMTMP) (t-stat = 3.06, p-value = 0.00), and curve number (CN2) (t-stat = 2.34, p-value = 0.01) were among the most sensitive parameters. The least sensitive parameters observed were the soil evaporation compensation factor (ESCO) (t-stat = 0.12, p-value = 0.90), initial soil water storage expressed as a fraction of the field capacity water content (FFCB) (t-stat=0.10, p-value = 0.92), and average slope length (SLSUBBSN) (t-stat = 0.00, p-value = 0.99). The p-stats value (average thickness of 95 Percent Prediction Uncertainty, PPU, divided by standard deviation) was 0.81, where a value close to 1 is considered reasonable [41]. After the values that best fit the observed data were determined, they were incorporated into SWAT. Simulations were performed for a continuous period from 1980 to 2000. The model performance was evaluated and revealed a satisfactory corelation between simulated and observed values for time steps monthly and daily time steps (Table 2). Figure 2 shows the hydrographs made for calibration and validation period for both daily and monthly time steps.

Table 2. Calibration and validation of stream flow simulated using Soil and Water Assessment Tool coupled with semi-automated SWAT-CUP.

Statistics	Calibration		Validation	
	(1987–1994)		**(1995–2000)**	
	Daily	**Monthly**	**Daily**	**Monthly**
NSE [†]	0.66	0.87	0.50	0.76
PBIAS	−21.45	−21.68	−2.87	−2.8
RMSE	7.045	3.56	5.93	3.25
R2	0.69	0.88	0.55	0.78

[†] NSE: Nash-Sutcliffe Efficiency; PBIAS: Percent bias; RMSE: Root mean square error, R^2: coefficient of determination.
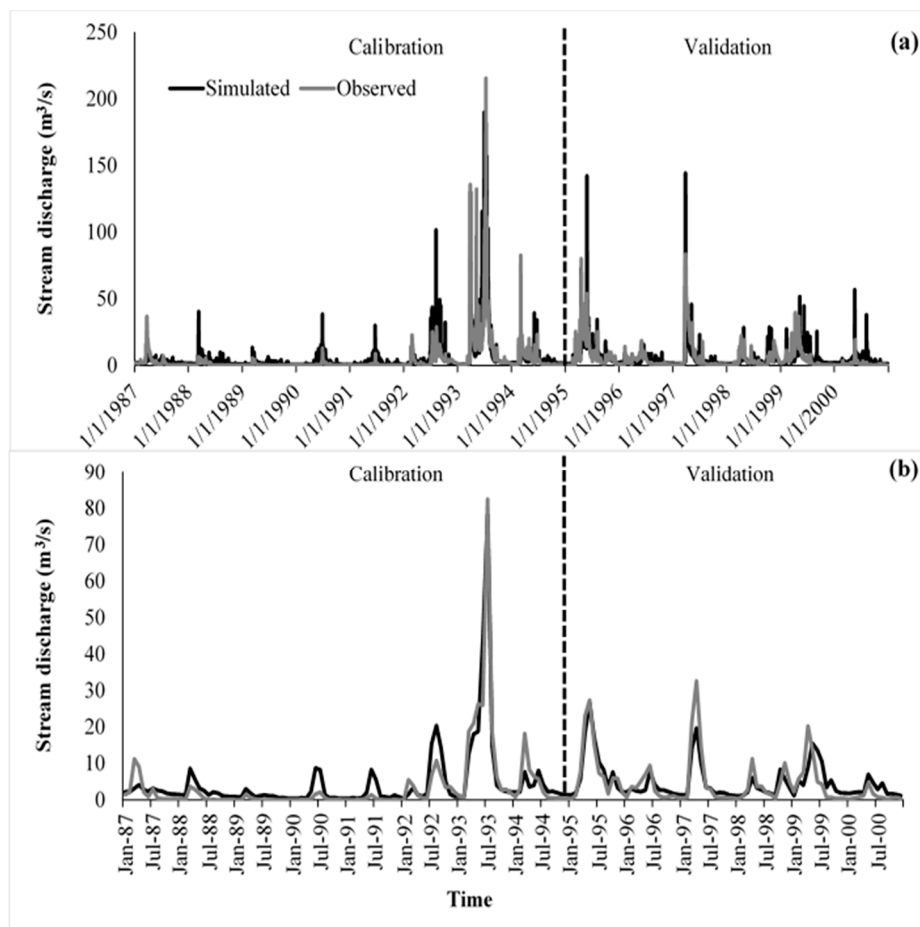
Figure 2. Hydrographs showing simulated and observed stream discharge (m³/s) during calibration and validation period at (**a**) daily; and (**b**) monthly time step for Skunk Creek watershed.

3.2. Projected Climate Condition

The analysis of bias-corrected future climate projections showed temperature increase in the range of 2.2 °C to 3.3 °C from baseline for all the three climate change scenarios. Seasonal decreases in temperature were observed in the winter. The largest decrease was found in A1B scenario, with a 30.5% reduction from baseline period. This was followed by a 29.5% reduction for the A2 scenario and a 19.0% reduction in the B1 Scenario during the winter. On the other hand, during the fall, a general increase in temperature was observed in all scenarios with increase of 32.2%, 41.3% and 44.3% for the B1, A2, and A1B scenarios, respectively (Tables A1, A2, A5 and A6).

Precipitation is projected to decline from the baseline to the mid-21st century for all scenarios. Maximum reduction could be seen in case of A2 (4.5%), followed by the A1B scenario (3.5%), and finally the B1 scenario (1.8%). The A2 scenario was projected to have a maximum reduction in precipitation during the summer months (−13.2%), a decline in precipitation was also observed for the spring (−5.3%) and fall (−7.2%) months. During the winter months, all three scenarios were projected to have an increase in precipitation from the baseline period to the mid-21st century. The A1B scenario had the largest increase in precipitation during the winter at 22.2%, followed by the B1 scenario (13.3%), and finally the A2 scenario (4.6%) (Figure 3).
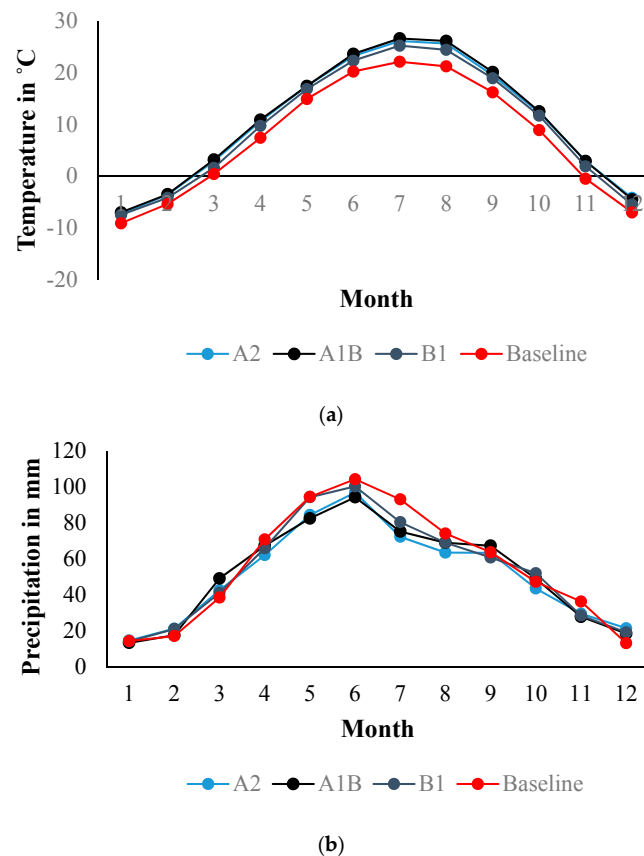
(**a**)

(**b**)

Figure 3. Monthly values observed for (**a**) temperature in °C; and (**b**) precipitation in mm for all three climate change scenarios and baseline time period.

3.3. Climate Change Impact on Hydrologic Processes

The various water balance components were estimated for baseline and each climate change scenario from the developed model and water budget was checked using fundamental equation

$$Precipitation = Run\ off + AET\ (Actual\ Evapotranspiration) + Storage \tag{9}$$

The error term or model bias was noticed to be somewhere from 5%–20 % for basline and climate change sceanrios. The values obtained in the baseline scenario and relative change noticed in the climate change scenarios expressed in percentage is depicted in Table 3.

Table 3. Water balance components observed for the baseline and relative changes noticed in percentage for different climate change scenarios.

	Precipitation	Actual ET	Water Yield (WYLD)	Soil Water (SW) Storage [†]
Baseline	665.80	614.30	72.80	−161.30
A2	−8.20	0.29	−91.07	−100.00
A1B	−10.00	−1.93	−91.21	−96.21
B1	−5.00	3.35	−86.69	−99.80

[†] Difference in soil water values from the beginning of simulation to the end of simulation was presented as the change in soil water storage. Negative values indicate loss in storage and vice versa.

The detailed explanation of impact of climate change on various water budget components is elucidated further in subsequent sections.

3.3.1. Snow Melt

Due to impact of climate change, snow melt values are expected to see a variation in different seasons in the mid-21st century. During the winter, there is projected to be a decrease in snow melt as temperature is expected to decrease, resulting in less melting. The A2 scenario (−43.06%) is projected to have the highest reduction in snow melt, followed by the B1 (−39.11%) and A1B (−37.64%) on an annual basis. During the spring, a decline in snow melt is projected for all scenarios with a reduction in the A2 scenario of −27.90%, a reduction in the A1B of −24.95% and a reduction in the B1 scenario of −2.46%. A reduction in snow melt is also projected in the fall with a maximum reduction in the A2 scenario (−57.50%) followed by the A1B scenario (−32.85%) and the B1 scenario (−39.08%). See Figures 4a and 5a, Tables A3 and A4.

Figure 4. Variations in different hydrologic components (**a**) Snowmelt, in mm; (**b**) Soil water storage (SW), in mm; (**c**) Actual evapotranspiration (AET), in mm; (**d**) Surface runoff (SURQ), in mm; € Total water yield (WYLD), in mm on seasonal basis in response to projected climate change scenarios.

3.3.2. Soil Water (SW) Storage

A reduction of 87%–91% in soil water storage is anticipated in all scenarios with A1B (−90.77%), A2 (−91.07%) and B1 (−87.92%). Soil water storage is expected to reduce least during the spring season in all climate change scenarios. With increased loss of water to the atmosphere and reduction in snowmelt, a reduction is observed in soil water storage for summer, fall, and winter. The sharp

decline in soil water storage in all seasons under all climate change scenarios with respect to baseline period can be attributed to the erratic pattern of rainfall including short events with high intensity precipitation and long dry spells (higher temperatures) with limited surface water resources during the mid-21st century that may lead to less soil permeability and hence limited soil water storage within soil profile. See Figures 4 and 5b, Tables A3 and A4.
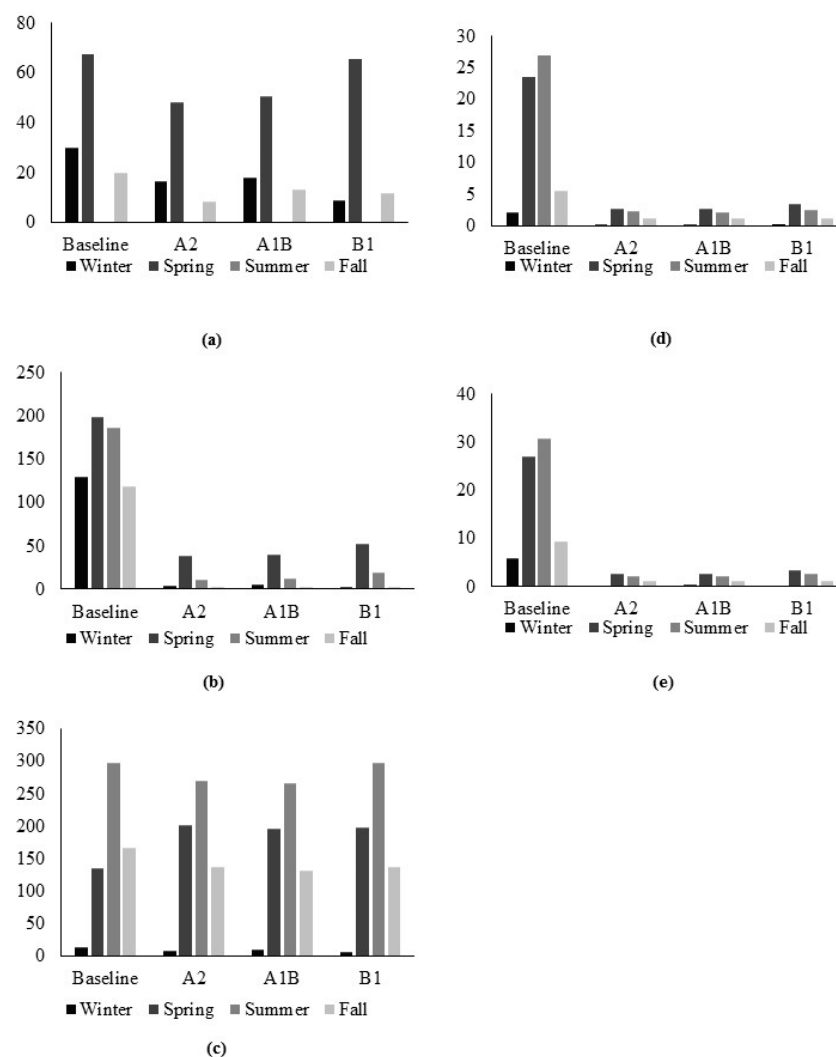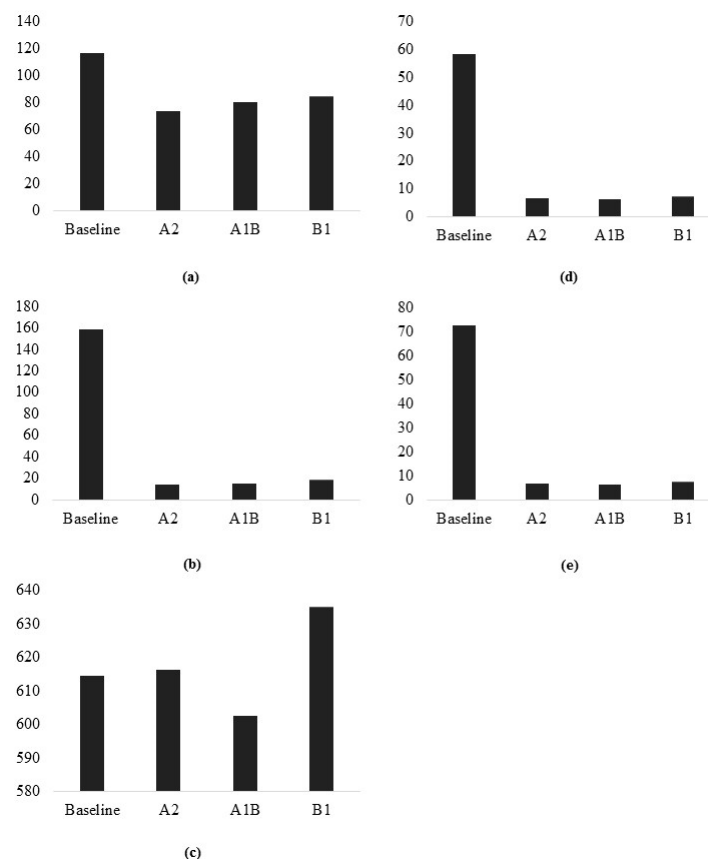

Figure 5. Variations in different hydrologic components (**a**) Snowmelt, in mm; (**b**) Soil water storage (SW), in mm; (**c**) Actual evapotranspiration (AET), in mm; (**d**) Surface runoff (SURQ), in mm; (**e**) Total water yield (WYLD), in mm on annual basis in response to projected climate change scenarios.

3.3.3. Actual Evapotranspiration (AET)

A nearly 50% increase in actual evapotranspiration is expected for all climate change scenarios during the spring, which indicates an environment with increased evapotranspirative losses leading to reductions in water availability during the spring months in the future. In the case of the A2 and A1B scenarios, a 34% and 37% increase in AET is projected in the winter months. In all other seasons and scenarios, AET is expected to decline. On an annual basis, an increase in AET ranging from 2% to 3% is projected in all climate change scenarios. See Figures 4c and 5c, Tables A3 and A4.

3.3.4. Surface Run-Off (SURQ)

Surface run-off is projected to decline to a large extent because of decrease in precipitation, increasing temperatures, and increasing ET losses projected by all three different climate change scenarios for Skunk Creek. The results show that the projected run-off for the winter months is very low in comparison to all other seasons which can be attributed to freezing temperatures during winters that causes more of precipitation to occur in solid snow. This can reduce the magnitude of total run-off. In addition, increasing evapotranspirative losses, more radiative influxes that contribute more water to atmosphere, and limited availability of precipitation may lead to low quantity of run-off for other

seasons as well. Similar to the seasonal pattern, run-off is also expected to decline on annual basis. Maximum reduction is projected to occur in the A2 scenario (−87.00%) followed by the A1B scenario (−84.87%) and B1 scenario (−83.46%). See Figures 4d and 5d, Tables A3 and A4.

3.3.5. Water Yield

A reduction of around 90%–92% in water yield (WYLD) is anticipated for all three climate change scenarios on an annual basis. A2 is expected to have the highest reduction (−91.6%) followed by A1B (−91.56%) and B1 (−90.67%) scenarios. Due to the projected decrease in snow melt during the winter months, it is likely that the total water yield will reduce during the winter in comparison to the baseline. However, during the spring and summer months, when much water is needed for crop growth, there is projected to be a decrease in the total water yield. Overall, winters summers are projected to be the most affected, followed by spring and fall. This is a concern for producers who will need to either look for an alternative water source or try to preserve and conserve current sources of water. See Figures 4e and 5e, Tables A3 and A4.

4. Discussion

The present study was conducted with an aim to assess the impact of climate change on the Skunk Creek watershed under different climate change scenarios laid down by SRES in mid-21st century. The purpose of choosing CMIP 3 SRES scenarios laid under IPCC AR 4 (Intercomparison Panel on Climate Change–Annual Report 4 over CMIP 5 (Coupled Modeled Intercomparison Project Phase 5) data laid under IPCC AR 5 was that there were some test runs going on with CMIP 5 data and the data to be used in hydrologic model needed to be bias-corrected and downscaled to RCM resolution. CMIP 5 data was available in 1-degree resolution, not downscaled and not bias-corrected, whereas CMIP 3 SRES scenarios were available at 0.25–degree resolution, downscaled and bias-corrected. Therefore, CMIP 3 was more reliable to be used than CMIP 5 at the time the research was conducted. For climate change scenarios we repeated the baseline precipitation and temperature data until the beginning of climate change scenario modeling years without which the model would have made the soil water completely dry and made the results unacceptable. Therefore, the soil water at the beginning of each climate change scenario was dry and went "very dry" at the end of simulation.

The estimates from the model assessed that a dry condition will predominate in the study area. The drier condition is expected due to sharp decline in the many hydrological components of the water cycle as simulated by SWAT. The decrease in hydrological components is attributed to the combined effect of decreasing precipitation and increasing temperatures (Tables A7 and A8). The assessment obtained in this study using SWAT are in line with many previous studies [13,40,41].

The combined effect of increases in temperature and reductions in precipitation in the mid-21st century within the Skunk Creek watershed will cause an increases in evapotranspiration. Possible reasons for the decline in precipitation are the changes in thermodynamic processes including the warming and moistening of the atmosphere, and the change in dynamic processes that deal with the circulation of air [42–45]. In addition to climatic factors, physiographic factors, geology, land use, and anthropogenic activities will compound the issues associated with the projected dry conditions of the mid-21st century. The projected precipitation changes strongly affect the variations in the quantity of hydrologic components like run off [42] in the future with more adversity being added by the rising temperatures in the watershed.

The results also indicate that there will be an increase in total energy availability with more net radiation and vapor pressure deficit, leading to high evapotranspirative losses with increases in temperature within the Skunk Creek Watershed [43]. An increase in surface net radiation can be attributed to forced anthropogenic greenhouse gases inhibiting long wave cooling, while an increase in vapor pressure deficit may result due to warming induced by greenhouse gases [44]. An increase in temperature may lead to more water losses as air temperature regulates the air moisture holding capacity and determines the potential water fluxes from soil to atmosphere [45]. More evaporative

losses due to warming and abundant energy availability will result in a drier environment [46]. Moreover, a reduction in the probability of having wet days during the crop growing season may be expected leading to higher probabilities of the occurrence of drought [47–54].

The SKW has observed alternate dry and wet periods for the last 15 years and this has altered the physical properties of soil and resulted in a decline in soil water storage. This occurrence can be explained by the fact that alternate dry and wet spells, along with short periods of high intensity precipitation, may contribute to the filling of surface pores and crust formation. This will lead to reduced infiltration. Permeability is also expected to decrease as pore spaces within the soil may become saturated, which in turn reduces the capacity further to store the water, resulting in little water storage. Also, the volume of pore space may become more limited [55].

In addition, elevated temperatures and erratic precipitation patterns will reduce snow melt in all seasons, leading to low flows and lower recharge to soil water. This leads to lower levels of water within the soil and limited water resources during crop growing season and will adversely affect irrigation demand as well as the crop productivity [56,57]. It was noticed that the baseline simulation showed approximately 11.5 mm reduction in soil water per year (161 mm reduction from 14-year simulation).The soil water values at the end of simulation was about 161 mm less than the beginning of simulation. The decrease in soil water storage have contributed to the water yield to some extent because precipitation (666 mm) is only 52 mm (666–614) in excess of ET for the baseline (Table 3). The remainder of decrease in soil water storage could have gone to groundwater, which we have not checked as the initial aquifer properties are subjected to many uncertainties for most of the watershed. The groundwater term used is with respect to deep aquifer losses not the sub-surface contributions to the flow. On the other hand, with a 55 mm reduction in precipitation and ET increased by two units, neither storage nor loss of water in soil profile resulted and the reduction in precipitation was reflected in the water yield for the A2 scenario. A similar trend was seen for B1 with the difference that there was slightly higher increase (of 20.6 mm) in ET compared to baseline. In the case of the A1B scenario, a reduction of 66 mm in precipitation was reflected mostly in water yield and to some extent in soil water storage with ET reduced by 11.9 mm and soil water storage reduced by 6.1 mm.

The soil moisture presented (−161 mm in 14 years) is the net change in monthly soil moisture totaled for all the years of simulation. We computed out monthly decrease (negative) or increase in soil moisture values and added them for all the years of simulation to find out whether there was net decrease or increase. We found a net decrease. The soil moisture went down all the way down to zero but recovered from the dry state in a couple of months. This occurred for a few years in the total simulation of 14 years from baseline (1987–2000). ET is related to soil moisture. When there is plenty of water in the soil profile, it will be used to meet the evaporative demand. But when supply from soil moisture store decreases ET is also reduced. Our seasonal summary of ET showed this trend. Soil moisture potential and average varies with type of soil. Within a sub-watershed they can vary widely.

All the projections of hydrologic processes under the three different climate change scenarios reveal that Skunk Creek will face an acute deficit of soil water storage within soil profile, surface run-off, snow melt, and total water yield, with an increase in ET losses. All these conditions are direct indicators of hydrological drought that may lead to a decline in agricultural productivity and may cause agricultural drought within the Skunk Creek watershed.

5. Conclusions

A SWAT model was built and its performance was evaluated in terms of NSE, R^2, PBIAS and RMSE, which revealed that there was strong corelation between simulated and observed stream flow for baseline period at monthly time step. The calibration process considered 24 different parameters. The purpose of using so many variables during calibration is to capture the influence of all the major factors dominant in the watershed to build a more reliable model to capture the variability of real world complexity within the watershed for better assessment of climate change impact studies.

The three different climate change scenarios studied were selected from the Special Report on Emission Scenarios (SRES) formulated by IPCC and included A2 (high emission), A1B (Medium Emission), and B1 (Low Emission). Overall, it was concluded that there will be a decline in soil water storage within soil profile, run-off and snow melt, with an acute reduction in water yield in the years between 2046 and 2065. This is caused by an increase in temperature, reduction in precipitation and rise in evaporative losses which are observed under all three scenarios. Therefore, dry conditions are projected to prevail in Skunk Creek under the impact of the climate change in the mid-21st century.

High pressure systems with elevated temperatures and expected prolonged warm and dry weather conditions with high radiation inputs and low humidity will enhance ET losses. Moreover, anomalies in weather conditions can lead to shifting snow melt patterns and low flow conditions are projected within the watershed for 2046 to 2065. If such a situation prevails, the actual growing season may decrease [58], and the mid-21st century may be badly afflicted with hydrologic and agricultural drought. The reduced water availability caused by climate change will negatively impact crop productivity. Hence it is important to estimate the quantity of existing water resources under the influence of the climate change [56,59].

Simulated projections from the current study indicate a similar trend in all cases with different degrees of severity for hydrological drought. Further studies are necessary to look for estimating the severity and extent of conditions that will prevail under different climate change scenarios. In addition, there is need to further understand and refine the projected climatic variables used to build future scenarios. It is so because the climate is the one of the important driving factors used in simulating the future hydrologic conditions within hydrologic models.

The same research can further be carried with Representative Concentration Pathways (RCPs) laid under IPCC AR 5, which may yield different results. RCP scenarios are now widely accepted over SRES scenarios. SRES Scenarios were widely used for hydrologic studies until mid-2015, when researchers validated that there was less uncertainty in predictions made by RCPs compared to SRES laid under IPCC AR 4. The differences in certainty between the two different predictions are due to the basis of laying future scenarios in RCPs being based on a different approach i.e., radiative forcing by 2100 to account for emissions, unlike in SRES, where factors driving emissions like population growth, economic growth, advances in technology etc, are used to estimate emissions. The future studies with RCPs may help in developing more resilient systems in mitigating the issues with water resources due to climate change impact.

There are many other dynamic factors like crop management practices and other man-made alterations within the watershed that affect the estimation of results. The data on those were not available, henceforth focus of this study was confined on better assessment than estimation. Furthermore, attention is required while selecting parameters during calibration and validation of the model using computer models. With the limitation of being computationally less extensive, computer-based hydrologic models need careful selection of parameters and ranges while the model is set up in order to make reliable estimates with better assessment of the hydrologic conditions under the different climatic change scenarios. Additionally, best management practices, such as incorporating heat tolerant or drought resistant varieties and modifying planting and harvesting dates to mitigate projected alterations in the hydrologic conditions of Skunk Creek during the mid-21st century can be tested further.

Author Contributions: Sushant Mehan designed the study, collected, and analyzed the data under the guidance of Narayanan Kannan and Rachel Mc Daniel. All the authors contributed substantially to the interpretation of results and editing the manuscript. The work is carried with the funding allotted to Sandeep Kumar under USDA-NIFA (Award No. 2014-51130-22593). Ram P. Neupane helped in intial development of model.

Conflicts of Interest: The authors declare no conflict of interest.

Appendix A

Table A1. Projected climate change scenarios (based on the Special Report on Emission Scenarios, SRES, IPCC 2007, CMIP 3 [†]) for the mid-21st century (2046–6205) in the Skunk Creek Watershed (SKW). (**a**) Change in annual and monthly temperature (magnitude) with respect to the baseline (1987–2000); (**b**) Change in annual and monthly precipitation (in percentage) with respect to the baseline (1987–2000).

SRES Scenarios	Month												Annual
(a)													
	January	February	March	April	May	June	July	August	September	October	November	December	
A2	1.7	1.8	2.5	3.2	2.5	3.0	4.0	4.4	3.3	3.4	3.5	2.8	3.0
A1B	2.1	2.0	2.9	3.5	2.5	3.4	4.5	4.9	3.9	3.6	3.4	2.5	3.3
B1	1.5	1.2	1.2	2.3	1.9	2.1	3.1	3.2	2.7	2.8	2.4	1.6	2.2
(b)													
	January	February	March	April	May	June	July	August	September	October	November	December	
A2	−6.7	3.0	27.7	−4.8	−12.7	−9.5	−19.3	−6.7	2.6	3.9	−23.5	41.4	−5.7
A1B	2.3	24.6	10.8	−12.3	−10.8	−7.1	−22.4	−14.2	−3.5	−7.7	−18.8	64.1	−8.0
B1	−1.6	23.0	6.6	−6.9	−0.3	−3.8	−13.7	−6.8	−7.5	10.2	−21.7	46.3	−3.4

[†] IPCC: Intergovernmental Panel on Climate Change; CMIP3: Coupled Model Intercomparison Project Phase 3.

Table A2. Seasonal variations in projected climate change scenarios (based on the Special Report on Emission Scenarios, SRES, IPCC 2007, CMIP 3 [†]) for the mid-21st century (2046–2065) in SKW, in percentage with respect to the baseline (1987–2000): (**a**) Temperature; (**b**) Precipitation.

Season	Special Report on Emission Scenarios, SRES, IPCC 2007, CMIP 3		
(a)			
	A2	**A1B**	**B1**
Winter (DJF)	−29.5	−30.5	−19.9
Spring (MAM)	36.3	39.4	23.7
Summer (JJA)	18.1	20.2	13.3
Fall (SON)	41.3	44.2	32.2
(b)			
	A2	**A1B**	**B1**
Winter (DJF)	11.2	29.0	22.0
Spring (MAM)	−2.3	−7.2	−1.3
Summer (JJA)	−12.1	−14.3	−8.0
Fall (SON)	−3.4	−8.6	−5.4

[†] IPCC: Intergovernmental Panel on Climate Change; CMIP3: Coupled Model Intercomparison Project Phase 3.

Table A3. Variation in different hydrologic components in percentage on monthly and annual time step compared to baseline in response to projected climate change scenarios.

SRES Scenarios	Month												Annual
(e)						Snowmelt							
	January	February	March	April	May	June	July	August	September	October	November	December	
A2	−100.00	−25.2	9.39	−100.00	−100.00	0.00	0.00	0.00	0.00	−100.00	−42.28	−58.64	−43.06
A1B	−73.55	−25.97	13.87	−100.00	−100.00	0.00	0.00	0.00	0.00	−100.00	−8.80	−57.29	−37.64
B1	−62.57	−73.60	44.58	−92.55	−100.00	0.00	0.00	0.00	0.00	−100.00	−17.26	−67.90	−39.11
(b)						Soil Water (SW)							
	January	February	March	April	May	June	July	August	September	October	November	December	
A2	−100.00	−91.47	−76.41	−81.18	−82.95	−87.72	−97.07	−98.85	−97.91	−97.53	−98.67	−99.93	−92.47
A1B	−98.98	−90.91	−76.01	−81.15	−82.12	−86.15	−97.62	−98.99	−98.11	−98.40	−97.98	−99.38	−92.15
B1	−98.76	−96.48	−69.27	−75.08	−75.16	−79.96	−93.38	−98.47	−98.17	−95.91	−99.32	−99.90	−89.99
(c)						Actual Evapotranspiration (AET)							
	January	February	March	April	May	June	July	August	September	October	November	December	
A2	−96.20	−15.92	140.02	60.75	14.62	19.83	−13.94	−30.35	−33.71	−6.60	34.92	−38.86	2.96
A1B	−69.09	−21.67	140.46	49.89	14.85	22.11	−13.21	−35.56	−35.32	−16.11	36.53	−35.14	3.14
B1	−62.04	−57.37	74.17	65.00	25.21	26.83	−0.09	−23.57	−37.03	−5.05	41.17	−60.20	−1.08
(d)						Surface Run Off (SURQ)							
	January	February	March	April	May	June	July	August	September	October	November	December	
A2	−100.00	−86.14	−87.05	−87.10	−90.85	−89.74	−94.42	−88.91	−78.98	−72.05	−84.55	−84.31	−87.00
A1B	−79.68	−84.49	−86.69	−89.49	−90.11	−88.68	−95.27	−89.90	−80.35	−79.72	−75.85	−78.29	−84.87
B1	−70.41	−96.64	−83.11	−86.21	−87.37	−87.43	−93.36	−88.87	−81.23	−65.83	−83.11	−79.92	−83.46
(f)						Water Yield (WYLD)							
	January	February	March	April	May	June	July	August	September	October	November	December	
A2	−99.82	−91.18	−88.41	−89.40	−91.81	−90.75	−94.95	−91.27	−85.35	−84.17	−93.77	−98.26	−91.60
A1B	−97.65	−90.15	−88.09	−91.35	−91.15	−89.79	−95.72	−92.04	−86.31	−88.49	−90.32	−97.66	−91.56
B1	−96.65	−96.55	−84.88	−88.68	−88.71	−88.68	−94.00	−91.23	−86.91	−80.67	−93.19	−97.82	−90.67

Table A4. Variation in different hydrologic components in percentage on seasonal basis compared to baseline in response to projected climate change scenarios.

Season	Special Report on Emission Scenarios, SRES, IPCC 2007, CMIP 3		
(a)	**Snowmelt**		
	A2	**A1B**	**B1**
Winter (DJF)	−44.94	−40.53	−70.53
Spring (MAM)	−27.90	−24.95	−2.46
Summer (JJA)	0.00	0.00	0.00
Fall (SON)	−57.50	−32.85	−39.08
(b)	**Soil Water (SW)**		
	A2	**A1B**	**B1**
Winter (DJF)	−96.83	−96.12	−98.26
Spring (MAM)	−80.39	−79.96	−73.37
Summer (JJA)	−93.98	−93.60	−89.65
Fall (SON)	−98.04	−98.16	−97.81
(c)	**Actual Evapotranspiration (AET)**		
	A2	**A1B**	**B1**
Winter (DJF)	−36.94	−34.05	−59.32
Spring (MAM)	48..29	44.70	45.16
Summer (JJA)	−9.80	−10.66	−0.35
Fall (SON)	−17.57	−21.26	−18.31
(d)	**Surface Run Off (SURQ)**		
	A2	**A1B**	**B1**
Winter (DJF)	−87.02	−83.77	−92.03
Spring (MAM)	−88.55	−88.60	−85.41
Summer (JJA)	−91.60	−91.74	−90.25
Fall (SON)	−77.64	−79.50	−76.72
(e)	**Water Yield (WYLD)**		
	A2	**A1B**	**B1**
Winter (DJF)	−94.97	−93.75	−96.87
Spring (MAM)	−89.94	−89.98	−87.19
Summer (JJA)	−92.62	−92.73	−91.43
Fall (SON)	−86.79	−87.88	−86.25

Table A5. Projected climate change scenarios (based on the Special Report on Emission Scenarios, SRES, IPCC 2007, CMIP 3 [†]) for the mid-21st century (2046–2065) in SKW. (**a**) Average annual and monthly temperature the baseline (1987–2000); (**b**) Cumulative annual and average monthly precipitation with baseline (1987–2000).

SRES Scenarios						Month							Annual
(a)													
	January	**February**	**March**	**April**	**May**	**June**	**July**	**August**	**September**	**October**	**November**	**December**	
Baseline	−9.1	−5.4	0.4	7.4	14.9	20.2	22.1	21.2	16.2	8.9	−0.5	−7.0	7.4
A2	−7.3	−3.6	2.9	10.6	17.4	23.2	26.1	25.6	19.5	12.3	2.9	−4.2	10.4
A1B	−7.0	−3.5	3.2	10.9	17.4	23.6	26.5	26.1	20.1	12.5	2.9	−4.5	10.7
B1	−7.6	−4.2	1.59	9.7	16.8	22.3	25.2	24.4	18.9	11.7	1.9	−5.5	9.6
(b)													
	January	**February**	**March**	**April**	**May**	**June**	**July**	**August**	**September**	**October**	**November**	**December**	
Basline	14.2	17.0	38.4	70.7	94.4	104.2	93.0	73.9	65.6	47.1	36.2	13.0	667.6
A2	13.2	17.5	49.0	67.2	82.4	94.2	75.1	69.0	67.2	48.9	27.7	18.3	629.8
A1B	14.5	21.1	42.5	62.0	84.2	96.8	72.2	63.4	63.3	43.4	29.4	21.4	614.1
B1	14.0	20.9	41.0	65.8	94.2	100.2	80.3	68.9	60.7	51.8	28.4	19.0	645

[†] IPCC: Intergovernmental Panel on Climate Change; CMIP3: Coupled Model Intercomparison Project Phase 3.

Table A6. Seasonal variations in projected climate change scenarios (based on the Special Report on Emission Scenarios, SRES, IPCC 2007, CMIP 3 [†]) for the mid-21st century (2046–2065) in SKW with the baseline (1987–2000): (**a**) Temperature; (**b**) Precipitation.

Season	Special Report on Emission Scenarios, SRES, IPCC 2007, CMIP 3			
(a)				
	Baseline	**A2**	**A1B**	**B1**
Winter (DJF)	−21.5	−15.2	−15.0	−17.3
Spring (MAM)	22.7	30.9	31.6	28.1
Summer (JJA)	63.4	74.9	76.3	71.9
Fall (SON)	24.6	34.8	35.5	32.5
(b)				
	Baseline	**A2**	**A1B**	**B1**
Winter (DJF)	44.1	49.0	56.9	53.8
Spring (MAM)	203.5	198.7	188.8	200.9
Summer (JJA)	271.1	238.2	232.3	249.4
Fall (SON)	148.8	143.9	136.1	140.9

[†] IPCC: Intergovernmental Panel on Climate Change; CMIP3: Coupled Model Intercomparison Project Phase 3.

Table A7. Seasonal Variations seen in scenarios B1 (with the combined effect of change in precipitation and temperature), BasePcpB1 (change in temperature), and Basetmp1 (change in precipitation) for the period from 2046–2065. The relative percentage change is with respect to the baseline.

	Absolute Magnitudes			Relative Percentage Change		
Snowmelt	**B1**	**BasePcpB1**	**Basetmp1**	**B1**	**BasePcpB1**	**Basetmp1**
Winter	8.9	1.0	30.6	−70.5	−96.7	1.6
Spring	65.6	78.9	70.3	−2.5	17.4	4.6
Summer	0.0	0.0	0.0	0.0	0.0	0.0
Fall	12.0	12.6	21.2	−39.1	−36.2	7.7
AET	**B1**	**BasePcpB1**	**Basetmp1**	**B1**	**BasePcpB1**	**Basetmp1**
Winter	5.8	5.1	13.8	−59.3	−63.9	−3.0
Spring	196.9	144.4	134.1	45.2	6.4	−1.1
Summer	296.8	328.6	299.5	−0.4	10.3	0.5
Fall	136.1	168.3	168.2	−18.3	1.0	1.0
WYLD	**B1**	**BasePcpB1**	**Basetmp1**	**B1**	**BasePcpB1**	**Basetmp1**
Winter	0.2	1.5	5.5	−96.9	−73.7	−5.6
Spring	3.5	12.5	26.0	−87.2	−53.6	−3.5
Summer	2.6	18.6	29.7	−91.4	−39.4	−3.2
Fall	1.3	5.9	8.8	−86.2	−36.8	−5.7
SW	**B1**	**BasePcpB1**	**Basetmp1**	**B1**	**BasePcpB1**	**Basetmp1**
Winter	6.8	240.5	407.0	−98.3	−38.1	4.7
Spring	158.2	525.8	622.3	−73.4	−11.5	4.7
Summer	57.8	442.0	573.8	−89.7	−20.9	2.8
Fall	7.8	228.1	369.8	−97.8	−35.7	4.2
SURQ	**B1**	**BasePcpB1**	**Basetmp1**	**B1**	**BasePcpB1**	**Basetmp1**
Winter	0.2	0.0	2.1	−92.0	−99.6	−3.3
Spring	3.4	11.1	22.9	−85.4	−53.1	−2.9
Summer	2.6	17.0	26.1	−90.2	−36.7	−3.0
Fall	1.3	4.3	5.1	−76.7	−21.2	−6.4

[†] BasePcpB1 represents the scenario B1 with no change in precipitation. Basetmp1 refers to the scenario B1 with no change in temperature.

Table A8. Annual variations seen in scenarios B1 (with the combined effect of change in precipitation and temperature), BasePcpB1 (change in temperature), and Basetmp1 (change in precipitation) for the period from 2046–2065. The relative percentage change is with respect to the baseline.

	Absolute Values			Relative Percentage Change		
	B1	**BasePcpB1**	**Basetmp1**	**B1**	**BasePcpB1**	**Basetmp1**
Snow Melt	84.5	92.5	117.2	−27.8	−21.0	0.1
AET	634.9	646.0	614.0	3.4	5.2	0.0
WYLD	7.5	38.0	68.7	−89.7	−47.8	−5.7
Soil Water Storage	229.0	1351.4	1835.8	−87.9	−28.7	−3.2
SURQ	7.5	32.4	56.1	−87.2	−44.3	−3.5

[†] BasePcpB1 represents the scenario B1 with no change in precipitation. Basetmp1 refers to the scenario B1 with no change in temperature.

References

1. Narsimlu, B.; Gosain, A.K.; Chahar, B.R. Assessment of future climate change impacts on water resources of upper Sind River basin, India using SWAT model. *Water Resour. Manag.* **2013**, *27*, 3647–3662. [CrossRef]
2. Ashraf, V.S.; Mousavi, S.J.; Abbaspour, K.C.; Srinivasan, R.; Yang, H. Analyses of the impact of climate change on water resources components, drought and wheat yield in semiarid regions: Karkheh River basin in Iran. *Hydrol. Pro.* **2014**, *28*, 2018–2032. [CrossRef]
3. Coulibaly, P.; Dibike, Y.B. *Downscaling of Global Climate Model Outputs for Flood Frequency Analysis in the Saguenay River System*; Canadian Climate Change Action Fund, Environment Canada: Hamilton, ON, Canada, 2004.

4.   Loukas, A.; Vasiliades, L.; Dalezios, N.R. Potential climate change impacts on flood producing mechanisms in southern British Columbia, Canada using the CGCMA1 simulation results. *J. Hydrol.* **2002**, *259*, 163–188. [CrossRef]

5.   Whitfield, P.H.; Cannon, A.J.; Reynolds, C.J. Modelling streamflow in present and future climates: Examples from the Georgia Basin, British Columbia. *Can. Water Resour. J.* **2002**, *27*, 427–456. [CrossRef]

6.   Cohen, S.; Kulkarni, T. *Water Management and Climate Change in the Okanagan Basin*; Environment Canada & University of British Columbia: Ottawa, ON, Canada, 2001.

7.   Cai, X.; Zeng, R.; Kang, W.H.; Song, J.; Valocchi, A.J. Strategic planning for drought mitigation under climate change. *J. Water Resour. Plan. Manag.* **2015**. [CrossRef]

8.   Chattopadhyay, S.; Jha, M.K. Hydrological response due to projected climate variability in Haw River watershed, North Carolina. *Hydrol. Sci. J.* **2014**. [CrossRef]

9.   MONDAL, A.; Mujumdar, P. Regional hydrological impacts of climate change: Implications for water management in India. In Proceedings of the International Association of Hydrological Sciences, Paris, France, 16–17 June 2014.

10. Mango, L.M.; Melesse, A.M.; McClain, M.E.; Gann, D.; Setegen, S.G. Land use and climate change impacts on the hydrology of the upper Mara River Basin, Kenya: Results of a modeling study to support better resource management. *Hydrol. Earth Syst. Sci.* **2010**, *15*, 2245–2258. [CrossRef]

11. Adem, A.A.; Tilahun, S.A.; Ayana, E.K.; Worqlul, A.W.; Assefa, T.T.; Dessu, S.B.; Melesse, A.M. Climate change impact on stream flow in the upper Gilgel Abay Catchment, Blue Nile Basin, Ethiopia. In *Landscape Dynamics, Soils and Hydrological Processes in Varied Climates*; Springer: Berlin/Heidelberg, Germany, 2016; pp. 645–673.

12. Gosain, A.; Rao, S.; Basuray, D. Climate change impact assessment on hydrology of Indian river basins. *Curr. Sci.* **2006**, *90*, 346–353.

13. Thomson, A.M.; Brown, R.A.; Rosenberg, N.J.; Izaurralde, R.C.; Legler, D.M.; Srinivasan, R. Simulated impacts of El Nino/southern oscillation on United States water resources. *J. Am. Water Resour. Assoc.* **2003**. [CrossRef]

14. Felzer, B.; Heard, P. Precipitation differences amongst GCMs used for the us national assessment. *J. Am. Water Resour. Assoc.* **1999**. [CrossRef]

15. Nijssen, B.; O'Donnell, G.M.; Hamlet, A.F.; Lettenmaier, D.P. Hydrologic sensitivity of global rivers to climate change. *Clim. Chang.* **2001**, *50*, 143–175. [CrossRef]

16. Jin, G.; Shimizu, Y.; Onodera, S.; Saito, M.; Matsumori, K. Evaluation of drought impact on groundwater recharge rate using SWAT and Hydrus models on an agricultural island in western Japan. *Proc. IAHS* **2015**, *371*, 143–148. [CrossRef]

17. Arnold, J.G.; Srinivasan, R.; Muttiah, R.S.; Williams, J.R. Large area hydrologic modeling and assessment Part I: Model development. *J. Am. Water Resour. Assoc.* **1998**. [CrossRef]

18. Arnold, J.G.; Srinivasan, R.; Neitsch, S.L.; Chris, G.; Abbaspour, C.; Gassman, P.W.; Fang, H.H.; van Griensven, A.; Debels, P.; Kim, N.W. *Soil and Water Assessment Tool (Swat): Global Applications*; Funny Publishing: Bangkok, Thailand, 2009; Volume 4, p. 415.

19. CoLab. *Colab: Project Integration—Change Control-Life Cycle Management*; USDA Coolaborative Software Development Laboratory: Washinton, DC, USA, 2006.

20. Fontaine, T.; Klassen, J.; Cruickshank, T.; Hotchkiss, R. Hydrological response to climate change in the Black Hills of South Dakota, USA. *Hydrol. Sci. J.* **2001**, *46*, 27–40. [CrossRef]

21. Pervez, M.S.; Henebry, G.M. Assessing the impacts of climate and land use and land cover change on the freshwater availability in the Brahmaputra River basin. *J. Hydrol. Reg. Stud.* **2015**, *3*, 285–311. [CrossRef]

22. Mosbahi, M.; Benabdallah, S.; Boussema, M.R. Assessment of soil erosion risk using SWAT model. *Arab. J. Geosci.* **2013**, *6*, 4011–4019. [CrossRef]

23. Phomcha, P.; Wirojanagud, P.; Vangpaisal, T.; Thaveevouthti, T. Predicting sediment discharge in an agricultural watershed: A case study of the Lam Sonthi watershed, Thailand. *Sci. Asia* **2011**, *37*, 43–50. [CrossRef]

24. Neupane, R.P.; Kumar, S. Estimating the effects of potential climate and land use changes on hydrologic processes of a large agriculture dominated watershed. *J. Hydrol.* **2015**. [CrossRef]

25. Neitsch, S.L.; Arnold, J.G.; Kiniry, J.R.; Williams, J.R. *Soil and Water Assessment Tool Theoretical Documentation*, version 2009; Texas Water Resources Institute: College Station, TX, USA, 2011.

26. Mockus, V. *National Engineering Handbook Section 4: Hydrology*; United States Department of Agriculture: Washington, DC, USA, 1972.

27. Shahidian, S.; Serralheiro, R.; Serrano, J.; Teixeira, J.; Haie, N.; Santos, F. *Hargreaves and Other Reduced-Set Methods for Calculating Evapotranspiration*; InTech: Princeton, NJ, USA, 2012.

28. Jensen, M.E.; Haise, H.R. Estimating evapotranspiration from solar radiation. *J. Irrig. Drain. Div.* **1963**, *89*, 15–41.

29. Wang, X.; Melesse, A.; Yang, W. Influences of potential evapotranspiration estimation methods on SWAT's hydrologic simulation in a northwestern Minnesota watershed. *Trans. ASAE* **2006**, *49*, 1755–1771. [CrossRef]

30. Thornton, P.E.; Running, S.W.; White, M.A. Generating surfaces of daily meteorological variables over large regions of complex terrain. *J. Hydrol.* **1997**, *190*, 214–251. [CrossRef]

31. Daymet: Daily Surface Weather on a 1 km Grid for North America, 1980–2008. Avaliable online: http://www.osti.gov/scitech/biblio/1149782 (accessed on 14 October 2016).

32. Oubeidillah, A.A.; Kao, S.C.; Ashfaq, M.; Naz, B.S.; Tootle, G. A large-scale, high-resolution hydrological model parameter data set for climate change impact assessment for the conterminous us. *Hydrol. Earth Syst. Sci.* **2014**, *18*, 67–84. [CrossRef]

33. Neupane, R.P.; White, J.D.; Alexander, S.E. Projected hydrologic changes in monsoon-dominated Himalaya Mountain basins with changing climate and deforestation. *J. Hydrol.* **2015**, *525*, 216–230. [CrossRef]

34. Keane, R.E.; Holsinger, L.M.; Parsons, R.A.; Gray, K. Climate change effects on historical range and variability of two large landscapes in western Montana, USA. *For. Ecol. Manag.* **2008**, *254*, 375–389. [CrossRef]

35. Nakicenovic, N.; Alcamo, J.; Davis, G.; De Vries, B.; Fenhann, J.; Gaffin, S.; Gregory, K.; Grübler, A.; Jung, T.Y.; Kram, T. *Special Report on Emissions Scenarios, Working Group III, Intergovernmental Panel on Climate Change (IPCC)*; Cambridge University Press: Cambridge, KY, USA, 2000.

36. Van Vuuren, D.P.; O'Neill, B.C. The consistency of IPCC's SRES scenarios to 1990–2000 trends and recent projections. *Clim. Chang.* **2006**, *75*, 9–46. [CrossRef]

37. Maurer, E.P.; Hidalgo, H.G.; Das, T.; Dettinger, M.; Cayan, D. The utility of daily large-scale climate data in the assessment of climate change impacts on daily streamflow in California. *Hydrol. Earth Syst. Sci.* **2010**, *14*, 1125–1138. [CrossRef]

38. Brekke, L.; Thrasher, B.; Maurer, E.; Pruitt, T. *Downscaled CMIP3 and CMIP5 Climate Projections: Release of Downscaled CMIP5 Climate Projections, Comparison with Preceding Information, and Summary of User Needs*; US Department of the Interior, Bureau of Reclamation: Denver, CO, USA, 2013.

39. Abbaspour, K. *SWAT-CUP 2012: Swat Calibration and Uncertainty Programs—A User Manual*; Eawag: Dübendorf, Switzerland, 2013.

40. Hamlet, A.F.; Lettenmaier, D.P. Effects of climate change on hydrology and water resources in the Columbia River Basin. *J. Am. Water Resour. Assoc.* **1999**. [CrossRef]

41. Zhang, X.; Zhang, L.; Zhao, J.; Rustomji, P.; Hairsine, P. Responses of streamflow to changes in climate and land use/cover in the Loess Plateau, China. *Water Resources Res.* **2008**. [CrossRef]

42. Chou, C.; Neelin, J.D.; Chen, C.A.; Tu, J.Y. Evaluating the "rich-get-richer" mechanism in tropical precipitation change under global warming. *J. Clim.* **2009**, *22*, 1982–2005. [CrossRef]

43. Chou, C.; Chiang, J.C.; Lan, C.W.; Chung, C.H.; Liao, Y.C.; Lee, C.J. Increase in the range between wet and dry season precipitation. *Nat. Geosci.* **2013**, *6*, 263–267. [CrossRef]

44. Held, I.M.; Soden, B.J. Robust responses of the hydrological cycle to global warming. *J. Clim.* **2006**, *19*, 5686–5699. [CrossRef]

45. Seager, R.; Naik, N.; Vecchi, G.A. Thermodynamic and dynamic mechanisms for large-scale changes in the hydrological cycle in response to global warming. *J. Clim.* **2010**, *23*, 4651–4668. [CrossRef]

46. Acton, Q.A. *Advances in Climate Change and Global Warming Research and Application*, 2012 ed.; ScholarlyEditions: Atlanta, GA, USA, 2012.

47. Scheff, J.; Frierson, D.M. Scaling potential evapotranspiration with greenhouse warming. *J. Clim.* **2014**, *27*, 1539–1558. [CrossRef]

48. Anderson, D.B. Relative humidity or vapor pressure deficit. *Ecology* **1936**, *17*, 277–282. [CrossRef]

49. Allen, R.G.; Pereira, L.S.; Raes, D.; Smith, M. *Crop Evapotranspiration—Guidelines for Computing Crop Water Requirements—FAO Irrigation and Drainage Paper 56*; FAO: Rome, Italy, 1998.

50. Cook, B.I.; Smerdon, J.E.; Seager, R.; Coats, S. Global warming and 21st century drying. *Clim. Dyn.* **2014**, *43*, 2607–2627. [CrossRef]

51. Keim, B.D.; Fontenot, R.; Tebaldi, C.; Shankman, D. Hydroclimatology of the US Gulf Coast under global climate change scenarios. *Phys. Geogr.* **2011**, *32*, 561–582. [CrossRef]
52. Wilby, R.L.; Wigley, T. Future changes in the distribution of daily precipitation totals across North America. *Geoph. Res. Lett.* **2002**, *29*, 31–39. [CrossRef]
53. Wehner, M.F. Predicted twenty-first-century changes in seasonal extreme precipitation events in the parallel climate model. *J. Clim.* **2004**, *17*, 4281–4290. [CrossRef]
54. Kharin, V.V.; Zwiers, F.W. Changes in the extremes in an ensemble of transient climate simulations with a coupled atmosphere-ocean GCM. *J. Clim.* **2000**, *13*, 3760–3788. [CrossRef]
55. Kharin, V.V.; Zwiers, F.W. Estimating extremes in transient climate change simulations. *J. Clim.* **2005**, *18*, 1156–1173. [CrossRef]
56. Kharin, V.V.; Zwiers, F.W.; Zhang, X. Intercomparison of near-surface temperature and precipitation extremes in AMIP-2 simulations, reanalyses, and observations. *J. Clim.* **2005**, *18*, 5201–5223. [CrossRef]
57. Semenov, V.; Bengtsson, L. Secular trends in daily precipitation characteristics: Greenhouse gas simulation with a coupled AOGCM. *Clim. Dyn.* **2002**, *19*, 123–140.
58. Voss, R.; May, W.; Roeckner, E. Enhanced resolution modelling study on anthropogenic climate change: Changes in extremes of the hydrological cycle. *Int. J. Climatol.* **2002**, *22*, 755–777. [CrossRef]
59. Eslamian, S. *Handbook of Engineering Hydrology: Fundamentals and Applications*; CRC Press: Boca Raton, FL, USA, 2014.